*Mathematical Biosciences and Engineering*

http://www.aimspress.com/journal/MBE

MBE, 18(6): 9511–9524.
DOI: 10.3934/mbe.2021467
Received: 21 June 2021
Accepted: 22 October 2021
Published: 01 November 2021

*Research article*

# Classification of gastric emptying and orocaecal transit through artificial neural networks

**Anibal Thiago Bezerra[1], Leonardo Antonio Pinto[2], Diego Samuel Rodrigues[3], Gabriela Nogueira Bittencourt[2], Paulo Fernando de Arruda Mancera[2] and José Ricardo de Arruda Miranda[2,*]**

[1] Institute of Exact Sciences, Federal University of Alfenas-MG (UNIFAL-MG), Alfenas-MG 37133-840, Brazil

[2] Institute of Biosciences, São Paulo State University (UNESP), Botucatu-SP 18618-689, Brazil

[3] School of Technology, University of Campinas (UNICAMP), Limeira-SP 13484-332, Brazil

* **Correspondence:** Email: jose.r.miranda@unesp.br.

**Abstract:** Classical quantification of gastric emptying (GE) and orocaecal transit (OCT) based on half-life time $T_{50}$, mean gastric emptying time (MGET), orocaecal transit time (OCTT) or mean caecum arrival time (MCAT) can lead to misconceptions when analyzing irregularly or noisy data. We show that this is the case for gastrointestinal transit of control and of diabetic rats. Addressing this limitation, we present an artificial neural network (ANN) as an alternative tool capable of discriminating between control and diabetic rats through GE and OCT analysis. Our data were obtained via biological experiments using the alternate current biosusceptometry (ACB) method. The GE results are quantified by $T_{50}$ and MGET, while the OCT is quantified by OCTT and MCAT. Other than these classical metrics, we employ a supervised training to classify between control and diabetes groups, accessing sensitivity, specificity, $f_1$ score, and AUROC from the ANN. For GE, the ANN sensitivity is 88%, its specificity is 83%, and its $f_1$ score is 88%. For OCT, the ANN sensitivity is 100%, its specificity is 75%, and its $f_1$ score is 85%. The area under the receiver operator curve (AUROC) from both GE and OCT data is about 0.9 in both training and validation, while the AUCs for classical metrics are 0.8 or less. These results show that the supervised training and the binary classification of the ANN was successful. Classical metrics based on statistical moments and ROC curve analyses led to contradictions, but our ANN performs as a reliable tool to evaluate the complete profile of the curves, leading to a classification of similar curves that are barely distinguished using statistical moments or ROC curves. The reported ANN provides an alert that the use of classical metrics can lead to physiological misunderstandings in gastrointestinal transit processes. This ANN capability of discriminating diseases in GE and OCT processes can be further explored and tested in other applications.

**Keywords:** gastric emptying; experimental diabetes mellitus; orocaecal transit; deep learning; artificial intelligence

## 1. Introduction

The gastrointestinal (GI) transit depends upon a coordinated association of mechanisms [1]. The two main processes to characterize the GI transit are gastric emptying (GE) and orocaecal transit (OCT). Several conditions may influence the GI transit, such as medications [2], meal composition [3], and pathologies such as diabetes mellitus [4]. Hyperglycemia, neuropathy and GI morphological alterations resultant from diabetes mellitus have been associated with abnormal GI motility, like disordered gastric motor function [5], and delayed GE [6] and OCT [7].

Usually, the likelihood of GI transit alterations in diabetic patients who show GI symptoms is performed qualitatively [8]. However, previous studies indicate that the analysis of the GI symptoms is not suitable for predicting GI transit alterations since these changes may be asymptomatic [9, 10]. Therefore, it is essential to identify abnormal GI transit in diabetic patients, once it may impair the glycemic control and the delivery of nutrients [11].

The GE is commonly measured by the $T_{50}$ value, defined as the time when the initial signal is decreased by 50% [12]. Furthermore, OCT may be quantified in terms of the orocaecal transit time (OCTT), defined as the first relevant signal detected in caecum [13, 14]. Both $T_{50}$ and OCTT are considered the gold standard parameters in clinical practice, but their results can be misleading in situations like irregularly shaped data profiles, because they are single values aimed to characterize the whole time series. Alternatively to $T_{50}$ and OCTT, Podczeck et al. [15] introduced statistical moments to quantify both GE and OCT in terms of mean gastric emptying time (MGET) and mean caecum arrival time (MCAT). These measures represent, respectively, the time when a mean amount of tracer is emptied from the stomach or arrived at the caecum and are given by

$$\text{MGET} = \frac{\int_0^{t_{\max_1}} t\, f_1(t)\, dt}{\text{AUC}}, \tag{1.1}$$

$$\text{MCAT} = \int_0^{t_{\max_2}} t\, f_2(t)\, dt, \tag{1.2}$$

where $f_1$ and $f_2$ are respectively the GE and OCT signals, $t_{\max}$ is the maximum time of a given signal, and AUC is the area under the curve of GE, being here both signals considered as a time-continuous curve. As a result, they are based on the whole measurement process, which may improve the data interpretation. However, since statistical moments are based on the curve profile, the noisiness of the signal plays an important role in the measurement and can lead to unreal quantifications.

Given the presented scenario and further contradictions of the classical metrics $T_{50}$, OCTT, MGET and MCAT, we address that the application of artificial neural networks (ANNs) on GE and OCT data can be suitable to detect GI transit alterations. It is well known that ANNs have been used

successfully in several areas of medicine [16], which include many recent applications for both diagnosing and prediction of diabetes [17–22]. Moreover, ANNs also have been widely applied in the field of gastroenterology in terms of diagnosis and prognosis [23–26]. However, most of these applications remain almost unexplored in GI transit disorders and diseases [27], lacking the opportunity to further explore and detect physiological changes caused by diabetes and other pathologies. Accordingly, by using gathered data from an experimental model of induction of diabetes mellitus that causes a disturbance in the GI transit, here we develop an ANN classifier capable of discriminating in the GI transit between control and diabetic rats based on GE and OCT measurements of non-digestible solids. The resulted ANN classification is then contrasted to the classical quantification of GE and OCT by the metrics $T_{50}$, OCTT, MGET and MCAT. As reported here, two out of four of these classical metrics were found to be significantly different in diabetic and control groups, but two of them do not. This inappropriate contradiction is circumvented in our ANN approach, which was able to detect changes in the gastrointestinal transit and to reveal still hidden characteristics of diabetes.

The paper is organized as follows. In Section 2, we present the methods of the study. In Section 3, we present our results, which are then discussed in Section 4. Finally, Section 5 closes the paper with some concluding remarks.

## 2. Materials and methods

### *2.1. Animals*

Male Wistar rats aged 30 days were obtained from São Paulo State University (UNESP) animals house, Botucatu, São Paulo State, Brazil. The rats were kept in a room with a controlled light/dark cycle of 12 h, temperature (24 ± 2 $^{o}$C) and humidity (60 ± 5 %), and they were fed ad libitum with a standard rat chow (Presence Nutrição Animal, Paulínia, Brazil). To the purpose of this study, they were randomly assigned into two groups: control ($n$ = 22) or diabetes ($n$ = 19). All experiments were conducted according to the UNESP Committee For the Use and Care of Animals (Protocol #752).

### *2.2. Induction of diabetes*

On the 90th day of age a single intraperitoneal injection of streptozotocin (STZ, 50 mg $kg^{-1}$, dissolved in citrate buffer solution, pH 4.5) was performed in diabetes group rats. Control group rats received an equal injected volume of vehicle. Three days after the induction, diabetes was verified by a blood glucose level of $\geq$ 200 mg $dL^{-1}$, measured using an Accu-Check glucometer (Performa, Roche, Germany) on blood taken from the tail vein [28]. Control rats presented a blood glucose of 87.64 ± 10.45 mg $dL^{-1}$ and diabetic rats presented a blood glucose of 401.40 ± 49.13 mg $dL^{-1}$ ($p < 0.0001$), confirming a successful induction of diabetes. Thus, the animals that were randomly assigned to the diabetic group developed this condition after induction. The reported fasting blood glucose tests also confirmed that rats of the control group were not diabetic.

### *2.3. Gastric emptying and orocaecal transit measurements*

Thirty days after induction, control and diabetic rats were submitted to GE and OCT assessment by the alternate current biosusceptometry (ACB), a noninvasive biomagnetic technique that has been

extensively applied to assess GI transit in rats [29–31]. Briefly, the ACB sensor consists of one pair of excitation coils and one pair of detection coils mounted in a coaxial arrangement. Each pair of excitation and detection coils is divided into two sub-systems: the reference and the measurement system. The reference system is placed far from the sample to subtract the environmental noise, while the measurement system is used to detect the signal from the magnetic material. The signal acquired by the ACB sensor depends on the amount and position of the magnetic material, which enables its application to assess GI transit in both rats and humans [29–32]. Detailed technical information was reported elsewhere [33].

Regarding the experiment, after a 12 h fast, rats were fed with a 2 g test meal composed of 0.5 g manganese ferrite ($MnFe_2O_4$) microparticles (size between 53 and 75 μm) incorporated into 1.5 g of standard rat chow. Manganese ferrite remains completely inert in all pH solutions and therefore cannot be absorbed by the GI tract [31]. Ten minutes after the test meal ingestion, rats were gently handled by the neck, and the ACB sensor was positioned on their gastric and caecum projections [29]. Measurements were repeated on the awake rats at the same points at intervals of 15 minutes for 6 hours. Therefore, the recorded data was composed of a time series of the electrical signal intensity for each animal in the control and case groups. The GE was classically quantified by $T_{50}$ and MGET, while the OCT was quantified using the OCTT and MCAT. Concerning the assessing of GE and OCT, the animal experimentation protocol presented here was already published before [29, 31, 34].

### *2.4. Statistical analysis for classical metrics of gastric emptying and orocaecal transit*

All GI parameters obtained by ACB measurements were expressed as mean ± standard deviation. Values of MGET, $T_{50}$, MCAT, and OCTT obtained from control and diabetic rats were compared using unpaired Student's t-test and ROC analyses. A statistically significant difference was considered at $p < 0.05$.

### *2.5. Neural network architecture*

Our inputs are time series data of ACB (GE and OCT) and our outputs are binary classification for either case (i.e., diabetes, 1) or control (0). With the ACB data, we then employ a dense feed-forward deep neural network, composed of input, hidden, and output layers to perform the classification between case (diabetic rats) and control (non-diabetic rats). It is implemented and trained using the TensorFlow engine with the Keras backend [35]. The classification task consists of passing the pre-classified ACB time-series to the network and ask it to retrieve the group that the animal owing such data belongs to.

For the classification task, we attempt to find the best neural network architecture by tuning its hyperparameters, namely, the number of hidden layers, the number of neurons per layer, the learning rate, the layer weight regularizer threshold, the activation functions, and the optimizer. The tuning process is done by enumeration, finding the set of parameters that leads to the higher accuracy. The network architecture is schematized in Figure 1. As a matter of representation, the colors and linewidths in the figure typify the layers' connections, the weights, and the groups. Some hyperparameters chosen for the training are presented in Table 1.

The choice of parameters and the training procedure are performed separately for the gastric emptying and the orocaecal arrival signals. However, both the GE and OCT inputs are chosen to be a

$20 \times 1$ column tensor, obtained from the ACB measurement. For the gastric emptying signal, the input layer is followed by two hidden layers with 52 neurons each. All hidden layers are activated with the rectified linear unit (ReLU) function, and it is added the L1 activity regularizer with a threshold of $10^{-5}$. The output layer is formed by a single neuron activated with the softmax function. Outputs are binarized as 1 to case (diabetes) and 0 to control.

For the orocaecal arrival signal, though, a shallower network is needed, composed of two hidden layers with 24 neurons each, also activated by the ReLU function and with the L1 regularizer with a threshold of $10^{-5}$. The output layer remains the same as that of gastric emptying data. Both ANNs employ the Stochastic Gradient Descent for training, compiled using the Adam optimizer [36] with a learning rate $l_r = 0.0005$. We apply the mean squared error as the loss and accuracy as the metric. After the training, the confusion matrix is evaluated, and neural networks' sensitivity, specificity, and $f_1$ score are retrieved.

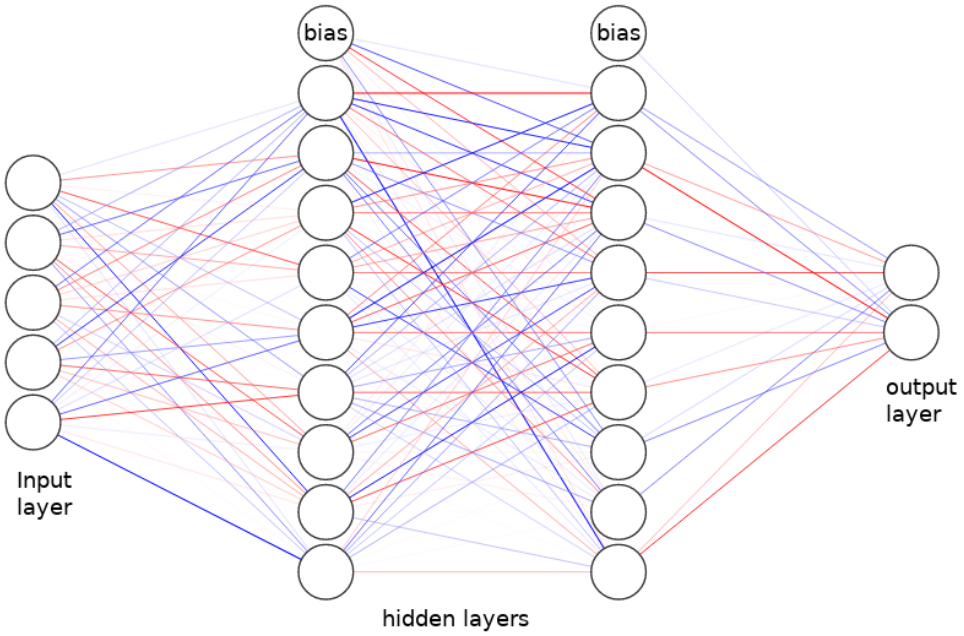


**Figure 1.** Representation of a dense neural network. Linewidths of connectors represent the weights: the wider the line, the heavier the weight. Blue color: control; red color: diabetes.

**Table 1.** Artificial Neural Network architecture, showing the number of neurons per layer as well as the activation function (ReLU and softmax). Output layer has only one binary neuron that returned 0 for control and 1 for case.

| Sample | Hidden 1 | | Hidden 2 | | Output | |
|---|---|---|---|---|---|---|
| | Neurons | Activation | Neurons | Activation | Neurons | Activation |
| GE | 52 | ReLU | 52 | ReLU | 1 | softmax |
| OCT | 24 | ReLU | 24 | ReLU | 1 | softmax |

As we mentioned, for the training and validation processes we have access to GE and OCT data from 41 samples distributed between case (19) and control (22). During the choice of hyperparameters, we

determine the use of about 3/4 of the samples for the training, and the remaining 1/4 for validation. As expected, for such a small dataset, the supervised training is challenging. Both the gastric emptying and orocaecal arrival classification require to deal with overfitting. It is a common bottleneck from neural networks related to ANNs memorizing the data set. To overcome such a problem, during the training procedure, the L1 regularization was applied as a standard way of decorrelating representations reducing overfitting [37–39]. In addition to that, we also use the early stop technique as an effective way of preventing overfitting [40], finishing the training procedure as soon as a chosen metric, namely the accuracy, ended changing.

### *2.6. Data standardization and normalization*

Working with neural networks usually requires a pre-processing step to the ANN to be able to better generalize. The ANN weights are normally initialized by small random numbers and a significant numeric difference between them and the inputs leads to inadequate training [41].

Since the raw data of gastric emptying is originally acquired as a time series from the ACB technique, to take advantage of the power of the ANN, the raw electric signal is standardized as to have a mean equals zero and a standard deviation of 1, according to

$$x_{\text{std}} = \frac{x - \langle x \rangle}{\sigma}, \tag{2.1}$$

where $x$ is the raw signal and $\sigma$ is its standard deviation. Figure 2 shows the standardized signal for both (a) the gastric emptying and (b) the orocaecal arrival. As one can observe, a visual classification between case and control is not clear, even though the OCT signal has a more pronounced variance in contrast to the GE signal, especially for later times.

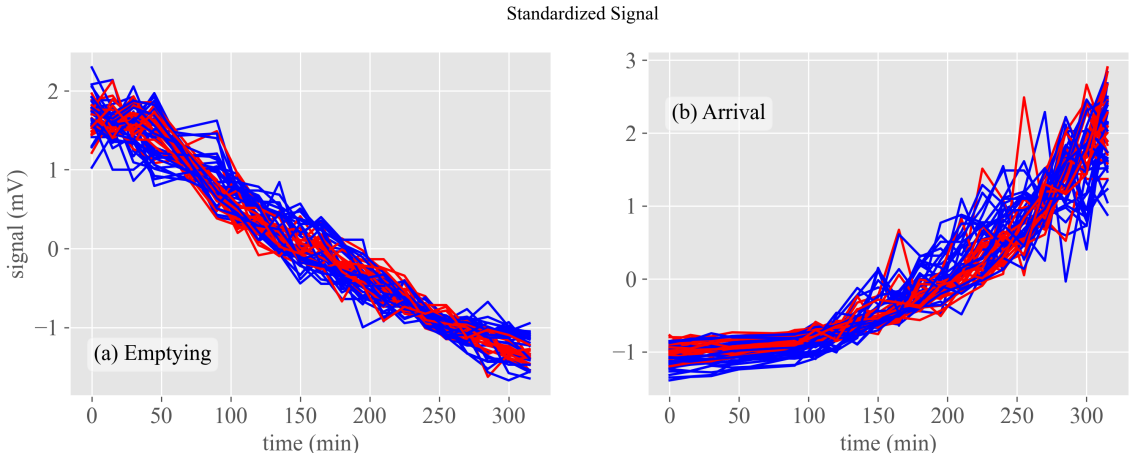


**Figure 2.** Experimental time series obtained by the alternate current biosusceptometry technique for (a) the gastric emptying and (b) the orocaecal arrival. Each curve refers to a specific rat with blue related to cases and red related to controls. The data were standardized according to the Eq (2.1).

## 3. Results

Table 2 shows the quantification obtained from ACB signals. The GE process is quantified by the gold standard parameter $T_{50}$ and the statistical moment MGET. While the MGET of diabetic rats is delayed in comparison to control ($p < 0.05$), $T_{50}$ quantification shows no differences between groups ($p = 0.28$). However, we found the opposite situation for the OCT quantification. The gold standard parameter OCTT is delayed in diabetic rats ($p < 0.0001$), but no differences are found for MCAT between control and diabetes group ($p = 0.31$).

**Table 2.** MGET, $T_{50}$, MCAT, and OCTT results for control and diabetic rats. Values are expressed as mean ± standard deviation. * $p < 0.05$ and ** $p < 0.0001$ vs. Control.

| Parameter | Control (n = 22) | Diabetic (n = 19) |
|---|---|---|
| MGET (min) | 97.27 ± 23.3 | 108.50 ± 5.2 * |
| $T_{50}$ (min) | 138.60 ± 24.5 | 145.80 ± 16.3 |
| MCAT (min) | 265.70 ± 9.7 | 271.90 ± 26.6 |
| OCTT (min) | 116.40 ± 17.9 | 145.50 ± 24.4 ** |

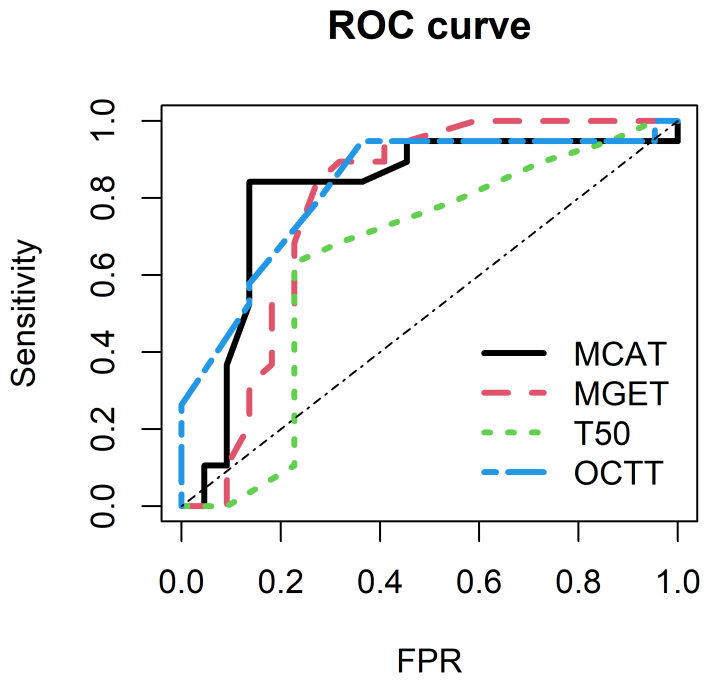


**Figure 3.** ROC curves for MCAT, MGET, $T_{50}$ and OCTT, with sensitivity in the y-axis and false positive rate (FPR) in the x-axis.

Figure 4(a) shows the training results for GE and Figure 4(b) shows the same for OCT. For GE, training accuracy starts at 40% and validation accuracy starts at 60%, both rising to 80–90% for epochs greater than 140. After 150 epochs, the network starts to overfit. Training accuracy reaches more than

90%, but the validation accuracy decreases. The ANN memorizes the piece of data used for the training; hence, the remaining of the data used only to evaluate the training is new to the network, and its classification becomes worse. Training loss and accuracy also show clues of overfitting after epoch 150. The early stop technique is then applied to prevent overfitting, finishing the training before it occurs. Thereby, for GE, the sensitivity is 88%, the specificity is 83%, and the $f_1$ score is 88%, showing that the supervised training and classification is successful.

Besides the statistics presented in Table 2, we proceed with the comparison of our results by reporting the value of AUROC (area under the receiver operator curve*) for both ANN and MGET, MCAT, $T_{50}$ and OCTT. By treating these latter also as binary classifiers, we get a receiver operating curve (ROC) for each of those metrics by using different thresholds. The referred curves are shown in Figure 3, where the straight line represents a binary random classifier. Classifiers with reasonable performances are those whose ROCs lie above this baseline†. This is the case only for the ROC curve of OCTT. At the other end of the performance, the poorest classification is the one given by $T_{50}$. This is consistent with the analysis based on the Student's t-test presented in Table 2. However, both of these analyses based on classical statistics turn out to be rather inconclusive.

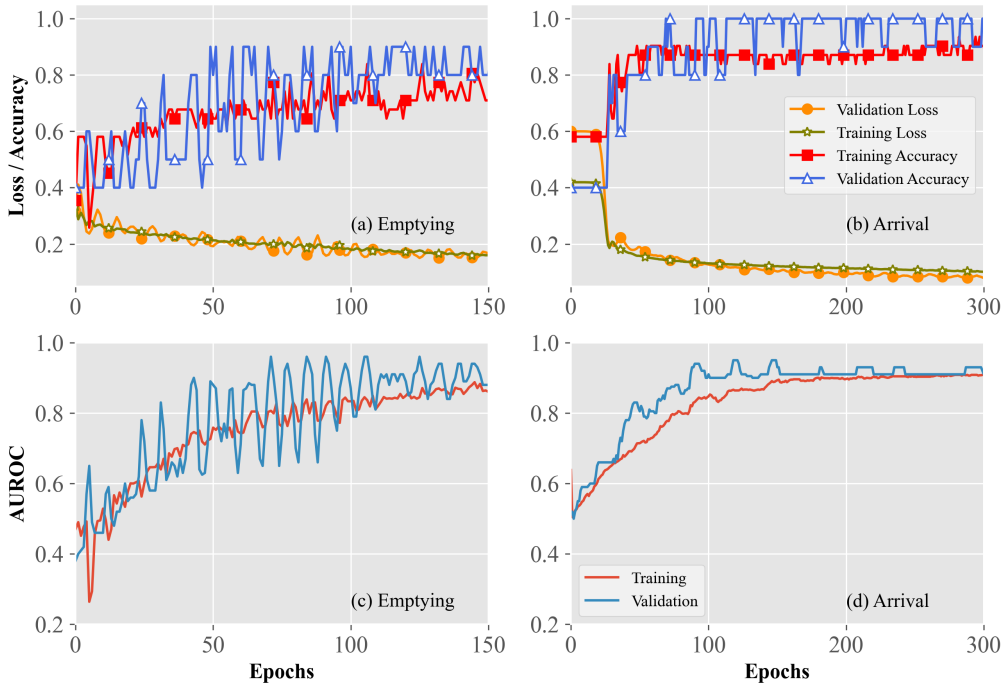


**Figure 4.** ANN training results for (a) GE and (b) OCT. Area under the receiver operating characteristic (AUROC) for (c) GE and (d) OCT.

In order to compare the performance of the referred binary classifiers, we report the AUROC value for each ROC shown in Figure 3: OCTT — 0.83; MCAT — 0.81; MGET — 0.79; T50 — 0.65.

*AUROC is a typical performance metric employed to evaluate the classification process [42, 43].
†For example, a perfect ROC curve is the one in which sensitivity reaches the level of 100% for a false positive rate (FPR) of 0.

Again, within this criterion, the best (OCTT) and the poorest ($T_{50}$) binary classifiers are in agreement with the preceding results. As a reference for the reader, the performance of binary classifiers can be seen in [44]. However, as we commented earlier, the shape of their ROC curves should also be taken into account. Keeping this limitation in mind, we now describe the accomplishments of our ANN methodology and its AUROC values for GE and OCT.

Figure 4 shows that the general trend of the training of GE (Figure 4(a)) and OCT (Figure 4(b)) are quite similar. However, due to the more considerable variance of the ACB signal for OCT in comparison to GE (see Figure 2), it is easy for the ANN to generalize the latter. Using a shallower neural network, though, we achieve an overall accuracy of about 90%, with losses of around 10%. The ANN also starts to overfit after epoch 300, and the training is early stopped to prevent it. The specificity is 75%, the sensitivity is unitary (100%), with a $f_1$ score of 85%. The training procedure for the OCT requires more epochs, but the results are better in comparison to GE, with no significant increase in the computational cost.

Figure 4(c) presents the AUROC metric evaluation for the training and validation process for GE. Figure 4(d) presents the AUROC metric for OCT. As one can observe, training and validation achieve AUROC values of about 0.9, demonstrating that the ANN accomplishes a better performance in comparison with classical metrics whose AUROCs are about 0.8 or less.

## 4. Discussion

There is a wide range of methodologies to assess GE and OCT [45]. In humans, scintigraphy is considered the gold standard method to measure GE [46], while the hydrogen breath test is used to evaluate OCT [47]. Due to practical challenges, techniques such as phenol red and activated charcoal are commonly employed to assess GE and OCT in animal studies, even though these techniques require an increased number of animals [48, 49]. In this context, the ACB method enables a non-invasive assessment of GE and OCT in both humans and animals [29, 32]. Due to distinct physical principles, the GI transit quantification may vary substantially depending on the chosen method. While the gold standard parameters $T_{50}$ and OCTT consider only a single value for representing complex processes such as GE and OCT, the statistical moments presented here confers the advantage of considering the whole measurements for quantification. However, our GI parameters quantification shown in Table 2 reveals an example of contradictions. Namely, OCTT is delayed in the diabetic group, but for $T_{50}$ no significant differences are found. Regarding the statistical moments, MGET is delayed in diabetic rats, but no significant differences between control and diabetes are found for MCAT.

As it is shown in Figure 2, GE and OCT curves from control and diabetic rats are very similar, and the parameter chosen to quantify the data lead to distinct interpretations. For instance, GE curves from control and diabetic rats present a matching profile, but their AUC is different. As a result, a statistically significant difference is found for MGET, but not for $T_{50}$. On the other hand, for OCT curves, a statistically significant difference is found for OCTT, but not for MCAT. Although these classical parameters are widely used in clinical and bench research [7, 31, 50], the reported AUROC values and the ROC curve analyses also confirm that classical metrics can perform poorly in the task of differentiating control and diabetic rats based on GI transit alterations. In the opposite direction, our ANN approach was able to detect differences even in a small dataset, revealing that further studies should be carried out focusing in terms of the GI physiology.

Regarding our number of samples, it can be thought of as small when compared to traditional artificial intelligence tasks, such as digit and image classifications, where the datasets easily overcome thousands of entries. From the medical point of view, an *a priori* data classification is challenging and not always feasible [51]. Therefore, efforts have been done to build up models able to reliable do the classification task. Accordingly, our results show that ANNs can generalize a small dataset [52–55]. In fact, as shown in Figure 4, the validation accuracy of the our ANN for both GE and OCT is about 80–90%, being comparable with other similar methodologies that use more consolidated features [56].

Despite the fact of being able to generalize small and noisy datasets, deep neural networks can perform non-linear transformations in a pure multidimensional space, which makes them as good as Random Forest classifiers with ensembles of low bias decorrelated trees. We also point out the increasing interest in training transferability, where a pre-trained model can be used as a start point for a new classification process. Having access to the pre-trained models—even the ones performed on small datasets—can be a powerful tool to compose a database aimed to generalize other small datasets with shared properties. Additionally, the training is based on binary classification, so the number of features to be learned is small in comparison to the number of inputs [57].

## 5. Final remarks

The ANN presented here is able to evaluate the complete profile of the ACB curves, leading to a classification of the data thoroughly. Classical metrics based on statistical moments and on $T_{50}$ and OCTT quantification proved to be inconclusive and/or contradictory between diabetic and control groups. However, our ANN performed as a reliable tool in the task of classification of similar curves profiles that were barely distinguished with statistical moments. Our ANN methodology provides an alert that the use of classical metrics ($T_{50}$, OCTT, MGET, and MCAT) can lead to physiological misunderstandings in gastrointestinal transit processes. Moreover, our ANN approach was able to detect changes in the gastrointestinal transit that may reveal still hidden characteristics of diabetes.

The reported ANN capability of discriminating diseases in GE and OCT processes can be further explored and tested in other applications, including the ones in GI transit. For example, it is worth mentioning that our results are based on non-digestible solids, and then our proposed ANN does not address cases of distinct phases of food or test meal compositions, which can be done in further studies. In this sense, our new approach has the potential for contributing to new applications in the GI area. As for future works, one could also consider combining the standard metrics (MCAT, MGET, T50, OCTT) in a logistic regression model, to devise an improved statistical model for classification. As a final remark, we emphasize the increasing interest in training transferability between small data sets. Having access to the pre-trained ANNs can be a powerful starting point tool to help generalizing other small datasets with common characteristics.

## Acknowledgments

DSR, JRM, and ATB thanks the financial support received from FAPESP (Grant #2020/05556-0, São Paulo Research Foundation), CNPq (National Council for Scientific and Technological Development), and INCT-FNA (National Institute of Science and Technology – Nuclear Physics and Applications).

## Conflict of interest

The authors declare no potential conflict of interests.

## References


1. J. D. Huizinga, W. J. E. P. Lammers, Gut peristalsis is governed by a multitude of cooperating mechanisms, *Am. J. Physiol.-Gastrointest. Liver Physiol.*, **296** (2009), G1–G8.
2. A. D. Suchitra, Relative efficacy of some prokinetic drugs in morphine-induced gastrointestinal transit delay in mice, *World J. Gastroenterol.*, **9** (2003), 779.
3. S. S. Davis, J. G. Hardy, M. J. Taylor, D. R. Whalley, C. G. Wilson, The effect of food on the gastrointestinal transit of pellets and an osmotic device (osmet), *Int. J. Pharm.*, **21** (1984), 331–340.
4. J. Yin, J. Chen, J. D. Z. Chen, Ameliorating effects and mechanisms of electroacupuncture on gastric dysrhythmia, delayed emptying, and impaired accommodation in diabetic rats, *Am. J. Physiol.-Gastrointest. Liver Physiol.*, **298** (2010), G563–G570.
5. M. Horowitz, R. Fraser, Disordered gastric motor function in diabetes mellitus, *Diabetologia*, **37** (1994), 543–551.
6. M. Park, M. Camilleri, Gastroparesis: Clinical update. CME, *Am. J. Gastroenterol.*, **101** (2006), 1129–1139.
7. S. Rana, A. Bhansali, S. Bhadada, S. Sharma, J. Kaur, K. Singh, Orocecal transit time and small intestinal bacterial overgrowth in type 2 diabetes patients from north india, *Diabetes Technol. Ther.*, **13** (2011), 1115–1120.
8. M. Camilleri, Diabetic gastroparesis, *New Engl. J. Med.*, **356** (2007), 820–829.
9. F. L. Iber, S. Parveen, M. Vandrunen, K. B. Sood, F. Reza, R. Serlovsky, et al., Relation of symptoms to impaired stomach, small bowel, and colon motility in long-standing diabetes, *Dig. Dis. Sci.*, **38** (1993), 45–50.
10. A. Keshavarzian, F. L. Iber and J. Vaeth, Gastric emptying in patients with insulin-requiring diabetes mellitus, *Am. J. Gastroenterol.*, **82** (1987), 29–35.
11. A. E. Bharucha, M. Camilleri, L. A. Forstrom, A. R. Zinsmeister, Relationship between clinical features and gastric emptying disturbances in diabetes mellitus, *Clin. Endocrinol.*, **70** (2009), 415–420.
12. K. Hveem, K. L. Jones, B. E. Chatterton, M. Horowitz, Scintigraphic measurement of gastric emptying and ultrasonographic assessment of antral area: relation to appetite, *Gut*, **38** (1996), 816–821.
13. K. D. Wutzke, W. E. Heine, C. Plath, P. Leitzmann, M. Radke, C. Mohr, et al., Evaluation of oro-coecal transit time: a comparison of the lactose-[13c,15n]ureide 13co2- and the lactulose h2-breath test in humans, *Eur. J. Clin. Nutr.*, **51** (1997), 11–19.
14. O. Baffa, R. B. Oliveira, J. R. A. Miranda, L. E. A. Troncon, Analysis and development of AC biosusceptometer for orocaecal transit time measurements, *Med. Biol. Eng. Comput.*, **33** (1995), 353–357.

15. F. Podczeck, J. M. Newton, K. Yuen, The description of the gastrointestinal transit of pellets assessed by gamma scintigraphy using statistical moments, *Pharm. Res.*, **12** (1995), 376–379.

16. Y. Fukuoka, Artificial neural networks in medical diagnosis, in *Computational Intelligence Processing in Medical Diagnosis*, Physica-Verlag HD, (2002), 197–228.

17. R. D. H. Devi, A. Bai, N. Nagarajan, A novel hybrid approach for diagnosing diabetes mellitus using farthest first and support vector machine algorithms, *Obes. Med.*, **17** (2020), 100152.

18. N. A. Apreutesei, F. Tircoveanu, A. Cantemir, C. Bogdanici, C. Lisa, S. Curteanu, et al., Predictions of ocular changes caused by diabetes in glaucoma patients, *Comput. Methods Programs Biomed.*, **154** (2018), 183–190.

19. N. Anton, E. N. Dragoi, F. Tarcoveanu, R. E. Ciuntu, C. Lisa, S. Curteanu, et al., Assessing changes in diabetic retinopathy caused by diabetes mellitus and glaucoma using support vector machines in combination with differential evolution algorithm, *Appl. Sci.*, **11** (2021), 3944.

20. P. B. M. Kumar, R. S. Perumal, R. K. Nadesh, K. Arivuselvan, Type 2: Diabetes mellitus prediction using deep neural networks classifier, *Int. J. Cognit. Comput. Eng.*, **1** (2020), 55–61.

21. R. A. Karim, I. Vassányi, I. Kósa, After-meal blood glucose level prediction using an absorption model for neural network training, *Comput. Biol. Med.*, **125** (2020), 103956.

22. J. Chaki, S. T. Ganesh, S. Cidham, S. A. Theertan, Machine learning and artificial intelligence based diabetes mellitus detection and self-management: A systematic review, *J. King Saud Uni.-Comput. Inf. Sci.*, 2020.

23. F. Pace, M. Buscema, P. Dominici, M. Intraligi, F. Baldi, R. Cestari, et al., Artificial neural networks are able to recognize gastro-oesophageal reflux disease patients solely on the basis of clinical data, *Eur. J. Gastroenterol. Hepatol.*, **17** (2005), 605–610.

24. E. Lahner, Possible contribution of advanced statistical methods (artificial neural networks and linear discriminant analysis) in recognition of patients with suspected atrophic body gastritis, *World J. Gastroenterol.*, **11** (2005), 5867.

25. J. C. Peng, Z. H. Ran, J. Shen, Seasonal variation in onset and relapse of IBD and a model to predict the frequency of onset, relapse, and severity of IBD based on artificial neural network, *Int. J. Colorectal Dis.*, **30** (2015), 1267–1273.

26. T. Takayama, S. Okamoto, T. Hisamatsu, M. Naganuma, K. Matsuoka, S. Mizuno, et al., Computer-aided prediction of long-term prognosis of patients with ulcerative colitis after cytoapheresis therapy, *PLOS ONE*, **10** (2015), e0131197.

27. Y. J. Yang, C. S. Bang, Application of artificial intelligence in gastroenterology, *World J. Gastroenterol.*, **25** (2019), 1666–1683.

28. X. Y. Wang, J. D. Huizinga, J. Diamond, L. W. C. Liu, Loss of intramuscular and submuscular interstitial cells of cajal and associated enteric nerves is related to decreased gastric emptying in streptozotocin-induced diabetes, *Neurogastroenterol. Motil.*, **21** (2009), 1095–e92.

29. C. C. Quini, M. F. Américo, L. A. Corá, M. F. Calabresi, M. Alvarez, R. B. Oliveira, et al., Employment of a noninvasive magnetic method for evaluation of gastrointestinal transit in rats, *J. Biol. Eng.*, **6** (2012).

30. M. F. Américo, R. G. Marques, E. A. Zandoná, U. Andreis, M. Stelzer, L. A. Corá, et al., Validation of ACB in vitro and in vivo as a biomagnetic method for measuring stomach contraction, *Neurogastroenterol. Motil.*, **22** (2010), 1340–e374.

31. M. F. F. Calabresi, C. C. Quini, J. F. Matos, G. M. Moretto, M. F. Americo, J. R. V. Graça, et al., Alternate current biosusceptometry for the assessment of gastric motility after proximal gastrectomy in rats: a feasibility study, *Neurogastroenterol. Motil.*, **27** (2015), 1613–1620.

32. J. R. Miranda, O. Baffa, R. B. de Oliveira, N. M. Matsuda, An AC biosusceptometer to study gastric emptying, *Med. Phys.*, **19** (1992), 445–448.

33. L. A. Corá, M. F. Américo, F. G. Romeiro, R. B. Oliveira, J. R. A. Miranda, Pharmaceutical applications of AC biosusceptometry, *Eur. J. Pharm. Biopharm.*, **74** (2010), 67–77.

34. J. F. Matos, M. F. Americo, Y. K. Sinzato, G. T. Volpato, L. A. Corá, M. F. F. Calabresi, et al., Role of sex hormones in gastrointestinal motility in pregnant and non-pregnant rats, *World J. Gastroenterol.*, **22** (2016), 5761.

35. M. Abadi, A. Agarwal, P. Barham, E. Brevdo, Z. Chen, C. Citro, et al., TensorFlow: Large-scale machine learning on heterogeneous systems, 2015. Available from: https://www.tensorflow.org.

36. D. P. Kingma, J. Ba, Adam: A method for stochastic optimization, preprint, arXiv:1412.6980.

37. M. Cogswell, F. Ahmed, R. Girshick, L. Zitnick, D. Batra, Reducing overfitting in deep networks by decorrelating representations, preprint, arXiv:1511.06068.

38. N. Srivastava, G. Hinton, A. Krizhevsky, I. Sutskever, R. Salakhutdinov, Dropout: A simple way to prevent neural networks from overfitting, *J. Mach. Learn. Res.*, **15** (2014), 1929–1958.

39. W. Zaremba, I. Sutkever, O. Vinyals, Recurrent neural network regularization, preprint, arXiv:1409.2329.

40. B. Jason, *Better Deep Learning: Train Faster, Reduce Overfitting, and Make Better Predictions*, Machine Learning Mastery, 2018.

41. C. M. Bishop, *Neural Networks for Pattern Recognition*, Oxford University Press, 1995.

42. A. Tahmassebi, A. H. Gandomi, I. McCann, M. H. Schulte, A. E. Goudriaan, A. Meyer-Baese, Deep learning in medical imaging: fMRI big data analysis via convolutional neural networks, in *Proceedings of the Practice and Experience on Advanced Research Computing*, ACM, (2018), 1–4.

43. J. A. Swets, Roc analysis applied to the evaluation of medical imaging techniques., *Invest. Radiol.*, **14** (1979), 109–121.

44. D. W. Hosmer Jr, S. Lemeshow, R. X. Sturdivant, *Applied Logistic Regression*, John Wiley & Sons, 2013.

45. L. A. Szarka, M. Camilleri, Methods for measurement of gastric motility, *Am. J. Physiol.-Gastrointest. Liver Physiol.*, **296** (2009), G461–G475.

46. F. N. Christensen, S. S. Davis, J. G. Hardy, M. J. Taylor, D. R. Whalley, C. G. Wilson, The use of gamma scintigraphy to follow the gastrointestinal transit of pharmaceutical formulations, *J. Pharm. Pharmacol.*, **37** (1985), 91–95.

47. S. V. Rana, A. Malik, Hydrogen breath tests in gastrointestinal diseases, *Indian J. Clin. Biochem.*, **29** (2014), 398–405.

48. M. Camilleri, D. R. Linden, Measurement of gastrointestinal and colonic motor functions in humans and animals, *Cell. Mol. Gastroenterol. Hepatol.*, **2** (2016), 412–428.

49. F. A. A. Gondim, J. R. V. da Graça, G. R. de Oliveira, M. C. V. Rêgo, R. B. M. Gondim, F. H. Rola, Decreased gastric emptying and gastrointestinal and intestinal transits of liquid after complete spinal cord transection in awake rats, *Braz. J. Med. Biol. Res.*, **31** (1998), 1605–1610.

50. M. Samsom, J. Vermeijden, A. Smout, E. van Doorn, J. Roelofs, P. van Dam, et al., Prevalence of delayed gastric emptying in diabetic patients and relationship to dyspeptic symptoms: A prospective study in unselected diabetic patients, *Diabetes Care*, **26** (2003), 3116–3122.

51. R. Keshari, S. Ghosh, S. Chhabr, M. Vatsa, R. Singh, Unravelling small sample size problems in the deep learning world, in *2020 IEEE Sixth International Conference on Multimedia Big Data (BigMM)*, IEEE, (2020), 134–143.

52. Y. Bengio, Practical recommendations for gradient-based training of deep architectures, in *Lecture Notes in Computer Science*, Springer Berlin Heidelberg, (2012), 437–478.

53. M. Olson, A. Wyner, R. Berk, Modern neural networks generalize on small data sets, in *Proceedings of the 32nd International Conference on Neural Information Processing Systems*, (2018), 3623–3632.

54. S. Lu, X. Shi, M. Li, J. Jiao, L. Feng, G. Wang, Semi-supervised random forest regression model based on co-training and grouping with information entropy for evaluation of depression symptoms severity, *Math. Biosci. Eng.*, **18** (2021), 4586–4602.

55. A. Vitale, R. Villa, L. Ugga, V. Romeo, A. Stanzione, R. Cuocolo, Artificial intelligence applied to neuroimaging data in parkinsonian syndromes: Actuality and expectations, *Math. Biosci. Eng.*, **18** (2021), 1753–1773.

56. A. Mujumdar, V. Vaidehi, Diabetes prediction using machine learning algorithms, *Procedia Comput. Sci.*, **165** (2019), 292–299.

57. S. Ingrassia, I. Morlini, Neural network modeling for small datasets, *Technometrics*, **47** (2005), 297–311.


AIMS Press